e-*Blood*

Gene expression profiling reveals the defining features of the classical, intermediate, and nonclassical human monocyte subsets

Kok Loon Wong,[1] June Jing-Yi Tai,[1] Wing-Cheong Wong,[2] Hao Han,[2] Xiaohui Sem,[1] Wei-Hseun Yeap,[1] Philippe Kourilsky,[1] and Siew-Cheng Wong[1]

[1]Singapore Immunology Network and [2]Bioinformatics Institute, Agency for Science, Technology and Research, Singapore

New official nomenclature subdivides human monocytes into 3 subsets: the classical ($CD14^{++}CD16^{-}$), intermediate ($CD14^{++}CD16^{+}$), and nonclassical ($CD14^{+}CD16^{++}$) monocytes. This introduces new challenges, as monocyte heterogeneity is mostly understood based on 2 subsets, the $CD16^{-}$ and $CD16^{+}$ monocytes. Here, we comprehensively defined the 3 circulating human monocyte subsets using microarray, flow cytometry, and cytokine production analysis. We find that intermediate monocytes expressed a large majority (87%) of genes and surface proteins at levels between classical and nonclassical monocytes. This establishes their intermediary nature at the molecular level. We unveil the close relationship between the intermediate and nonclassic monocytes, along with features that separate them. Intermediate monocytes expressed highest levels of major histocompatibility complex class II, GFRα2 and CLEC10A, whereas nonclassic monocytes were distinguished by cytoskeleton rearrangement genes, inflammatory cytokine production, and CD294 and Siglec10 surface expression. In addition, we identify new features for classic monocytes, including AP-1 transcription factor genes, CLEC4D and IL-13Rα1 surface expression. We also find circumstantial evidence supporting the developmental relationship between the 3 subsets, including gradual changes in maturation genes and surface markers. By comprehensively defining the 3 monocyte subsets during healthy conditions, we facilitate target identification and detailed analyses of aberrations that may occur to monocyte subsets during diseases. (*Blood*. 2011; 118(5):e16-e31)

Introduction

Much of what is known about human monocyte heterogeneity is based on 2 subsets subdivided according to CD14 and CD16 expression.[1-8] However, it is becoming increasingly apparent that further monocyte heterogeneity exists.[9-15] The new nomenclature that subdivides monocytes into 3 subsets has recently been approved by the Nomenclature Committee of the International Union of Immunologic Societies.[16] Based on this new nomenclature, the major population of human monocytes (~ 90%) with high CD14 but no CD16 expression ($CD14^{++}CD16^{-}$) are now termed classical monocytes, whereas the minor population (~ 10%) of human monocytes are further subdivided into the intermediate subset, with low CD16 and high CD14 ($CD14^{++}CD16^{+}$), and the nonclassical subset, with high CD16 but with relatively lower CD14 expression ($CD14^{+}CD16^{++}$). This new nomenclature presents new challenges to the understanding of monocyte heterogeneity. For example, it is unclear how properties ascribed to total $CD16^{+}$ monocytes are segregated between the intermediate and nonclassical subset.

It has been proposed that the intermediate subset is a transitional population bridging between the classical and nonclassical monocyte subsets.[16,17] In macrophage colony-stimulating factor–treated patients, intermediate monocytes were expanded before the nonclassical subset.[18] The intermediate subset was shown to express a handful of surface markers at levels between the classical and nonclassical subsets.[4,9,19] In addition, controversy about the nonclassical subset exists. Nonclassical monocytes were shown to exhibit patrolling behavior in vivo and react strongly to nucleic acids and viruses.[9] But one rather surprising find was that the nonclassical subset responded poorly to lipopolysaccharide (LPS), which contradicts previous reports on the strong inflammatory response of the nonclassical subset toward LPS.[10,20]

Recently, Cros et al performed a microarray study on 4 human monocyte subsets, with the additional subset derived from dividing the nonclassical monocytes into $SLAN^{+}$ and $SLAN^{-}$ subsets.[9] These data were analyzed together with the mouse $Ly6C^{high}$ and $Ly6C^{low}$ monocyte subsets. Their clustering results showed a closer association between the human classical, intermediate, and mouse $Ly6C^{high}$ monocytes, irrespective of CD16 expression by the human intermediate subset. In contrast, another recent microarray study by Ingersoll et al[21] demonstrated that CD16 expression by human monocytes defines their homology to mouse $Ly6C^{low}$ monocyte subsets. Analysis of the 3 monocyte subsets in macaque monkeys also showed a closer association of the intermediate subset to the nonclassical, rather than to the classical subset.[22] Overall, the relationships described for the monocyte subsets thus far have been conflicting.

A proper biologic and functional definition of the 3 monocyte subsets during healthy conditions is essential for the understanding of monocyte subsets in diseases. For this, we analyzed the 3 circulating human monocyte subsets from healthy donors using extensively validated microarray, flow cytometry, and cytokine production analysis. We unveil the relationship of the 3 monocyte

Submitted December 20, 2010; accepted May 20, 2011. Prepublished online as *Blood* First Edition paper, June 7, 2011; DOI 10.1182/blood-2010-12-326355.

The online version of this article contains a data supplement.

The publication costs of this article were defrayed in part by page charge payment. Therefore, and solely to indicate this fact, this article is hereby marked "advertisement" in accordance with 18 USC section 1734.

subsets and describe unique features for each of the 3 monocyte subsets. Our study comprehensively defines the 3 monocyte subsets under normal healthy conditions, which will be useful for identifying features that may be altered during disease conditions. This will be particularly useful to clinical studies of diseases associated with monocytosis and/or conditions associated with changes in the proportion of monocyte subsets.

Methods

Purification of blood monocyte subsets

All blood samples and procedures in this study were approved by the Institutional Review Board, Singapore in accordance to guidelines of the Health Sciences Authority of Singapore. Informed consent was given in accordance to the Declaration of Helsinki. Peripheral blood mononuclear cells were obtained from blood of healthy donors using Ficoll density centrifugation and then depleted of NK and granulocytes using anti-CD56 and anti-CD15 conjugated microbeads by magnetic-automated cell sorting (Miltenyi Biotec). Monocyte subsets were then identified using anti-CD14 (clone 61D3) and anti-CD16 (clone 3G8). The 3 monocyte subsets (classical, intermediate, and nonclassical) were sorted using fluorescence-activated cell sorting (FACS), according to their relative expression of CD14 and CD16 as shown in Figure 1A. Sorted subsets were stored in Trizol at −80°C before RNA isolation.

Microarray processing and analysis

RNA was isolated from the sorted monocyte subsets using Qiagen RNeasy mini kit. RNA quality was confirmed using the QIAxcel analyzer (QIAGEN). A total of 300 ng of total RNA was processed using Illumina TotalPrep RNA Amplification Kit. Hybrization was performed on Illumina Human-6 Version 2 expression BeadChips. A total of 24 expression profiles were obtained, from the 3 monocyte subsets of 4 donors in duplicates. Readings were directly exported from Illumina BeadStudio and normalized using the procedures as described in Wong et al.[23] To obtain differentially expressed genes, analysis of variance (ANOVA) followed by the Tukey Honestly Significant Difference test ($P < .05$) was applied to obtain genes. After removing hypothetical genes, 1554 differentially expressed genes satisfied the criteria of $P < .05$, and ≥ 1.5-fold change for at least one comparison between the subsets. Hierarchical clustering and Principle component analysis were performed using Cluster Version 3.0 and Java Treeview.

Real-time PCR

Primers were sequences were given in supplemental Table 1 (available on the *Blood* Web site; see the Supplemental Materials link at the top of the online article). cDNA from purified monocyte subsets of healthy donors was obtained by reverse transcription using TaqMan Reverse Transcription reagents (Applied Biosystems). Real-time PCR was performed with ITAQ SYBR Green (Bio-Rad) using ABI7900 (Applied Biosystems). Each sample was analyzed in triplicates and normalized to the HPRT housekeeping gene.

Flow cytometry

Surface marker expression was determined using antibodies given in supplemental Table 2. Peripheral blood mononuclear cells from healthy donors were used and monocyte subsets were identified using CD14 and CD16 (Figure 1A). To prevent nonspecific binding, staining was performed in phosphate-buffered saline containing 5% (vol/vol) human serum and 5% (vol/vol) fetal calf serum. After 30 minutes of incubation in the dark at 4°C, labeled cells were washed once and analyzed using LSRII (BD Biosciences). For nonconjugated antibodies, labeling was performed first with the primary antibodies, washed, followed by the appropriate antimouse or antirabbit IgG fluorescent conjugates, washed, and followed by anti-CD14 and CD16 staining. Specific staining was determined using fluorescence minus one isotype or secondary only controls. Doublets were excluded using FSC-A versus FSC-H plots, and dead cells were excluded with 7-aminoactinomycin D (BioLegend). At least 200 000 total events were collected and analyzed with FlowJo software Version 7.6.1 (TreeStar).

Cytokine production

A total of 5×10^4 FACS-sorted classical, intermediate, and nonclassical monocyte subsets were seeded into 96-well round bottom plates in triplicates with 200 μL RPMI and 10% fetal bovine serum. Increasing doses of LPS from *Escherichia coli* 0111:B4 (Sigma-Aldrich) were added to the monocyte subset cultures. After 18 hours, supernatants were harvested and the levels of cytokines and chemokines were determined using Bio-Plex human cytokine assay kits (Bio-Rad). Samples were processed according to the manufacturer's instructions, and readings were obtained using Luminex 200 (Bio-Rad).

Results

The close relationship between the intermediate and nonclassical monocyte subset

First, we find that the proportion of the monocyte subsets from the mean ± SD of 16 healthy donors was 84.8% ± 5.6% for classical, 5.4% ± 1.9% for intermediate, and 9.2% ± 4.4% for the nonclassical subset. The classical, intermediate, and nonclassical monocyte subsets from the blood of 4 such healthy donors were purified using FACS as shown in Figure 1A. The resulting purity of these subsets was at least 97%. We obtained the gene expression profiles of these 3 monocyte subsets using Illumina BeadChip arrays (data deposited in GEO, accession number GSE25913). To determine the relationship between the 3 monocyte subsets, we subjected the complete dataset to hierarchical clustering (Figure 1B) and principle component analysis in an unbiased manner (Figure 1C). Both analyses showed that the intermediate and nonclassical monocytes were most closely clustered, whereas the classical and nonclassical were most distantly clustered.

To obtain differentially expressed genes, ANOVA followed by the Tukey Honestly Significant Difference test was applied to the dataset. After filtering out hypothetical genes, we obtained a list of 1554 differentially expressed genes with $P < .05$ and ≥ 1.5-fold differences for at least one of the possible comparisons between 2 subsets, classical versus nonclassical, classical versus intermediate, or intermediate versus nonclassical. Within these 1554 genes, the number of comparisons with ≥ 1.5-fold differences for classical versus nonclassical was 1456, intermediate versus classical was 942, and between intermediate versus nonclassical was 249 (Figure 1D). Hence, the number of genes that differ by ≥ 1.5-fold was the lowest between the intermediate and nonclassical subset. Therefore, similar conclusions about the relationship between the 3 subsets were reached with clustering of the whole dataset or analysis of the differentially expressed gene list.

We extensively validated our microarray results using monocyte subsets sorted from donors that were different from those that contributed to the microarray. The expression of a large panel of genes from the microarray was tested using real-time PCR (Figure 2). These genes are shown according to the highest expression by the classical (Figure 2A), intermediate (Figure 2B), and nonclassical subset (Figure 2C). Validation at the protein level was also performed by flow cytometric analysis of surface receptors (described later in Figures 6 and 7). Hence, even though the validation experiments were performed with donors distinct from those that contributed to the microarray, the

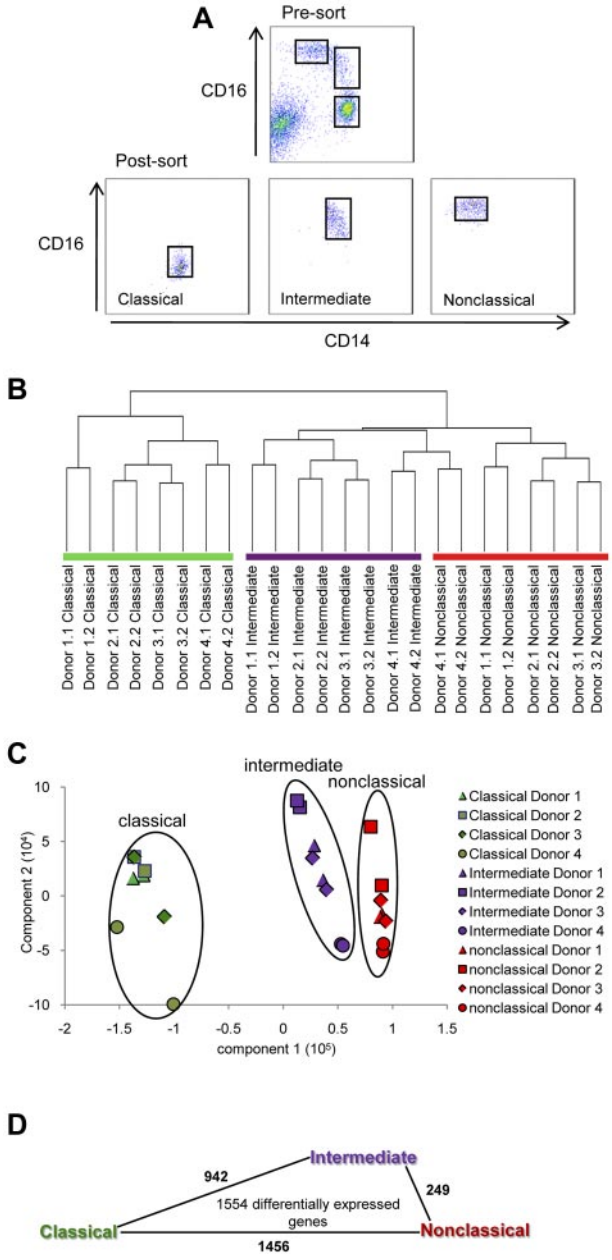

Figure 1. Purification of human monocyte subsets and microarray analysis. (A) The classical ($CD14^{++}CD16^{-}$), intermediate ($CD14^{++}CD16^{+}$), and nonclassical monocyte ($CD14^{+}CD16^{++}$) subsets were purified from 4 healthy donors using FACS. RNA was obtained and gene expression profiling was performed using Illumina Human-6 Version 2 BeadChip arrays. Duplicate samples for each donor were analyzed. (B) Gene expression profiles were subjected to hierarchical clustering using city block distance, average linkage (C) and principle component analysis. Shapes represent expression profiles of the different donors in duplicate. The different monocyte subsets are circled and are represented by different colors. Green, purple, and red represent the classical, intermediate, and nonclassical subset, respectively. (D) Number of comparisons with ≥ 1.5-fold change within the 1554 differentially expressed genes. The length of the lines between 2 monocyte subsets is proportional to the number of such comparisons.

validation experiments and microarray results were highly consistent.

Hierarchical clustering of genes reveals the transitional state of the intermediate subset

Next, we subjected the 1554 differentially expressed genes to unsupervised hierarchical clustering, which revealed 6 distinct clusters (Figure 3A). Clusters I and II were composed of 862 genes most highly expressed by the classical subset. Clusters III and IV were composed of 135 genes most highly expressed by the intermediate subset. Clusters V and VI were composed of 557 genes most highly expressed by the nonclassical subset. These gene lists with median intensity values and the relative fold changes normalized to the intermediate subset were given in supplemental Table 3. The top 50 genes most highly expressed by the classical, intermediate, and nonclassical subsets based on fold change values are shown in Tables 1, 2, and 3 respectively. As expected, *CD14*, *CCR2*, and *SELL* were within the most highly expressed genes for classical monocytes, whereas *FCGR3B*, *CX3CR1*, and *ITGAL* were most highly expressed for the nonclassical monocytes.

We noted that, although the intermediate subset was composed of the least number of highly expressed genes (135 of 1554 genes, 8.7%), they expressed a large majority of the differentially expressed genes at levels between the classical and nonclassical subset (1349 of 1554 genes, 87%). This could also be clearly visualized through the heat map (Figure 3A) seen as extensive blacked-out areas for the intermediate subset. This pattern of gene expression by the intermediate monocyte subset is supportive of the notion that this subset is an intermediary population between the classical and nonclassical subsets.[16,18]

Unique characteristics for the 3 monocyte subsets revealed by in silico analysis

We wanted to discover the unique characteristics of each monocyte subset based on their gene expression profiles. The 1554 differentially expressed genes ($P < .05$, ≥ 1.5-fold change) were divided according to the subset with the highest expression and analyzed for categories with significant enrichment ($P < .05$) of categories in Gene Ontology (GO) biologic processes using DAVID tools.[24] Similar categories were grouped. The *P* value of each group was given as the geometric means of the *P* values of the categories of each group (supplemental Table 4). In Figure 3B through D, we show representative groups and the relative $\log_2$ fold change of associated genes normalized to the intermediate subset.

For the classical subset, we found significant enrichment in categories under angiogenesis, wound healing, and coagulation, implicating them in tissue repair functions (Figure 3B). Several categories under the response to stimuli, including responses to bacterial components, toxins, drugs, hormones, hypoxia, and nutrient levels, were also found. Notably, proinflammatory mediators *S100A12*, *S100A9*, and *S100A8*[25] were among the top 50 most highly expressed genes for the classical subset (Table 1). Overall, this revealed that the classical monocytes are highly versatile, capable of responding to a variety of external cues to mediate tissue repair or immune functions.

For intermediate monocytes, significant enrichment for genes under major histocompatibility complex (MHC) class II processing and presentation were found (Figure 3C). This included 6 of these genes for α- and β-chains of MHC class II, and also 2 genes, *CD74* (class II invariant chain) and *HLA-DO*, which are involved in MHC class II antigen processing. The costimulatory molecule *CD40* was also most highly expressed by the intermediate subset.

For nonclassical monocytes, we found enrichment in categories involving cytoskeleton rearrangement (Figure 3D). Under cell movement, Rho GTPases RhoC and RhoF coordinate actin cytoskeleton rearrangement, providing the driving force for cell movement.[26] Their activators *VAV2* and *ARHGEF18* and downstream effectors *PIP5K2A* and *PKN1* were also most highly expressed by

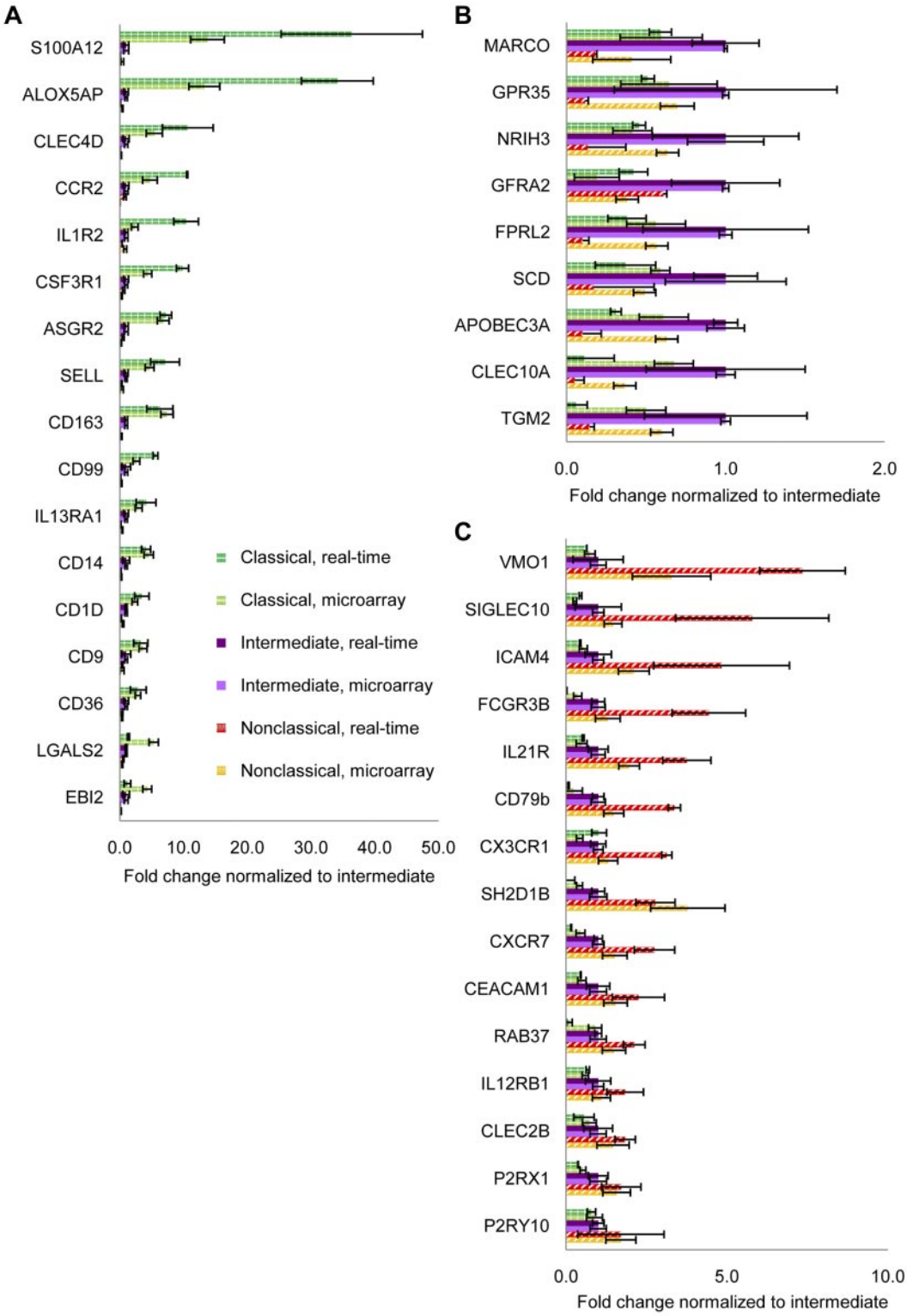

Figure 2. Validation of microarray data by real-time PCR. Real-time PCR was used to validate results from microarray. Genes were sorted according to the highest expression by (A) classical (green hatched bars), (B) intermediate (purple bars), and (C) nonclassical subsets (red striped bars). Real-time PCR results are shown in darker shades and expressed as mean ± SEM of 3 to 7 independent donors. Microarray results are in lighter shades and expressed as median ± SD of 4 independent donors.

the nonclassical subset. The relatively higher expression levels of these genes may explain the molecular basis of their highly motile patrolling behavior observed in vivo.[9] Another process involving cytoskeleton rearrangement was Fc receptor (FcR)–mediated phagocytosis. These included genes of the Src family kinase *LYN* and *HCK*, which phosphorylate immunoreceptor tyrosine-based activation motifs of FcRs, leading to the recruitment of *PIK3AP1*, *PIK3CG*, *LCP2*, and *CBL*. These FcR complexes activate *WASP2*, *VASP*, *PLCG2*, and *CORO2A*, leading to cytoskeleton remodeling necessary for phagocytosis.[27] Several complement component genes, including *C1QA*, *C1QB*, *C2*, and *C3*, were also most highly expressed by the nonclassical subset.

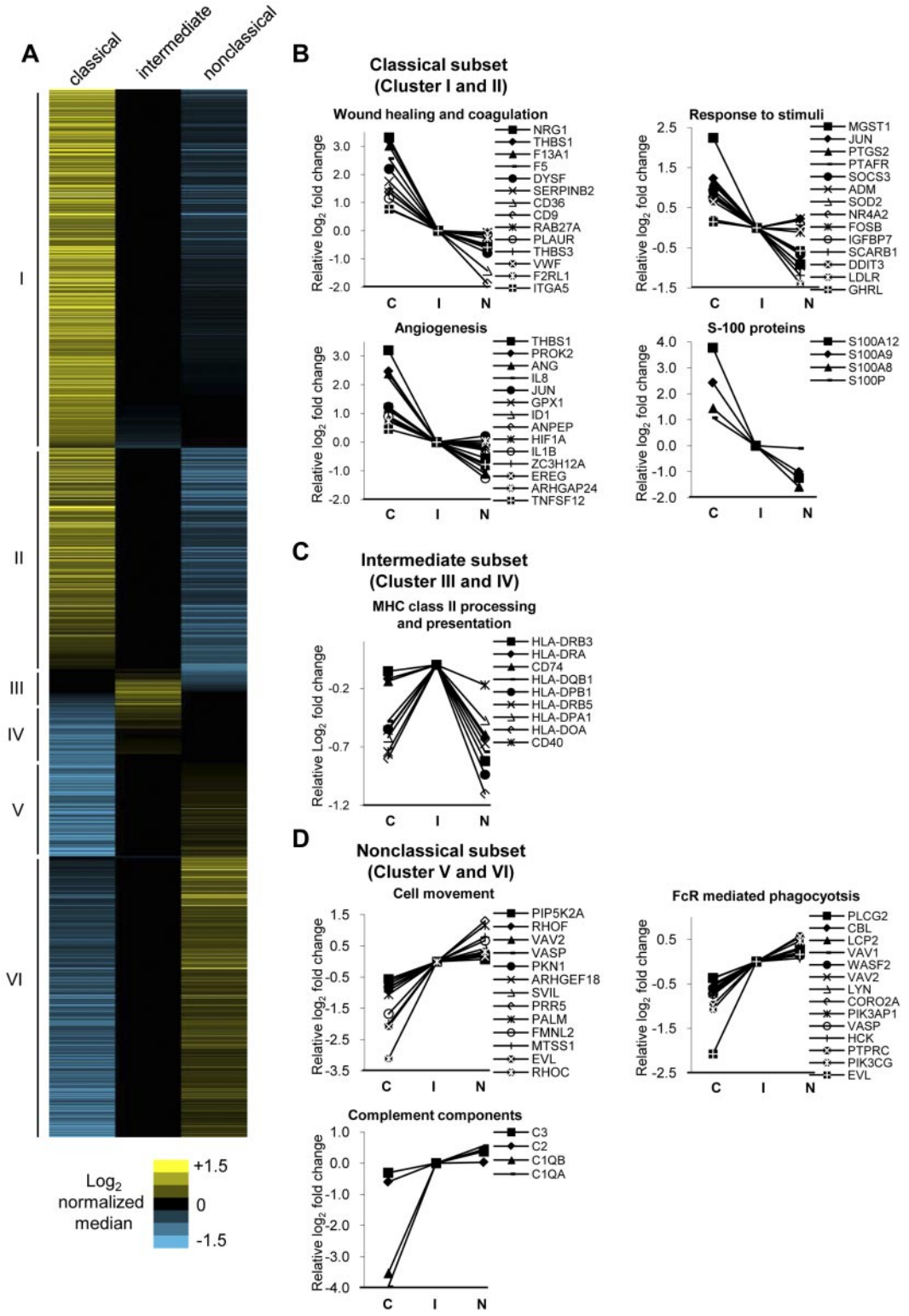

Figure 3. Hierarchical clustering of differentially expressed genes and the representative GO categories associated with the genes most highly expressed by each monocyte subset. (A) Hierarchical clustering using city block distance and average linkage of the 1554 differentially expressed genes ($P < .05$, fold change ≥ 1.5) reveals 6 distinct clusters. Clusters I and II are composed of 862 genes most highly expressed by the classical subset, clusters III and IV with 135 genes most highly expressed by the intermediate subset, and clusters V and VI with 557 genes most highly expressed by the nonclassical subset. The relative $\log_2$ fold change for each gene is shown by the corresponding heat maps. The most highly expressed genes from each subset were analyzed for enrichment of categories in Gene Ontology biologic processes using DAVID tools. Representative categories and associated genes enriched for the (B) classical, (C) intermediate, and (D) nonclassical subset are shown. The $\log_2$ levels of associated genes normalized to the intermediate subset are shown and listed according to decreasing MFI for the classical monocyte subset. C indicates classical monocyte subset: I, intermediate monocyte subset; and N, nonclassical monocyte subset.

Table 1. Top 50 genes most highly expressed by the classical monocyte subset sorted by decreasing absolute fold change values

	Fold change normalized to intermediate*	
Gene name	Classic	Nonclassic
S100 calcium binding protein A12 (S100A12)	13.76	−2.35
Arachidonate 5-lipoxygenase-activating protein (ALOX5AP)	13.27	−2.38
Peptidyl arginine deiminase type IV (PADI4)	10.08	−2.19
Neuregulin 1 (NRG1)	9.94	−1.40
mast cell-expressed membrane protein 1 (MCEMP1)	9.93	−2.93
Thrombospondin 1 (THBS1)	9.25	−1.46
Cysteine-rich secretory protein LCCL domain containing 2 (CRISPLD2)	8.79	−1.61
Coagulation factor XIII A1 polypeptide (F13A1)	8.14	−1.53
MOCO sulphurase C-terminal domain containing 1 (MOSC1)	7.81	−1.73
Cytochrome P450 family 27 subfamily A polypeptide 1 (CYP27A1)	7.61	−2.22
CD163 antigen (CD163)	7.42	−3.44
Glutaminyl-peptide cyclotransferase (QPCT)	7.31	−2.32
ADAM metallopeptidase domain 19 (ADAM19)	7.28	−1.54
Asialoglycoprotein receptor 2 (ASGR2)	6.82	−1.89
Ribonuclease RNase A family 2 (RNASE2)	6.31	−2.66
Coagulation factor V (proaccelerin labile factor; F5)	5.92	−1.44
Folate receptor 3 (gamma; FOLR3)	5.82	−2.32
Ribonuclease RNase A family 4 (RNASE4)	5.72	−1.58
Aldehyde dehydrogenase 1 family member A1 (ALDH1A1)	5.70	−2.51
Endothelial differentiation sphingolipid G-protein-coupled receptor 3 (EDG3)	5.57	−1.25
Prokineticin 2 (PROK2)	5.52	−1.87
C-type lectin domain family 4 member D (CLEC4D)	5.42	−1.34
S100 calcium binding protein A9 (calgranulin B; S100A9)	5.38	−2.03
Oncostatin M (OSM)	5.36	−2.27
Chondroitin sulfate proteoglycan 2 (CSPG2)	5.34	−3.98
Lectin galactoside-binding soluble 2 (GALS2)	5.33	−2.51
Angiogenin ribonuclease RNase A family 5 (ANG)	5.26	−2.14
Vanin 2 (VNN2)	5.21	−1.34
Epstein-Barr virus-induced gene 2 (EBI2)	4.31	−5.13
Urotensin 2 (UTS2)	5.06	−1.75
Ribonuclease P RNA component H1 (RPPH1)	4.76	−1.38
Microsomal glutathione S-transferase 1 (MGST1)	4.75	−1.88
Interleukin 8 (IL-8)	4.74	−1.08
Chemokine C-C motif receptor 2 (CCR2)	4.73	−1.25
Selectin L (SELL)	4.68	−1.84
Dysferlin limb girdle muscular dystrophy 2B (DYSF)	4.58	−1.72
Metallothionein 1F (MT1F)	4.57	−1.36
CD14 antigen (CD14)	4.54	−4.29
Ribonuclease RNase A family k6 (RNASE6)	3.72	−4.44
Colony-stimulating factor 3 receptor (CSF3R)	4.38	−1.62
Stabilin 1 (STAB1)	2.55	−4.35
Cytochrome P450 family 1 subfamily B polypeptide 1 (CYP1B1)	4.31	−1.16
Alcohol dehydrogenase iron containing 1 (ADHFE1)	4.29	−1.15
Phospholipase A2 group VII (PLA2G7)	4.27	−2.98
Matrix metallopeptidase 25 (MMP25)	4.14	−1.30
Zinc finger protein 395 (ZNF395)	4.11	−1.57
Solute carrier family 2 member 3 (SLC2A3)	3.78	−3.96
Early growth response 1 (EGR1)	3.79	−2.26
CKLF-like MARVEL transmembrane domain containing 2 (CMTM2)	3.78	−1.15
CD9 antigen p24 (CD9)	2.60	−3.66

*Obtained by calculating the MFI values of classical or nonclassical relative to intermediate.

Progressive increase in maturation status by the monocyte subsets

GO categories that reveal the relative differentiation state of the monocyte subsets were grouped under proliferation, cell differentiation, and apoptosis (Table 4). Classical monocytes were represented by genes that indicate an antiapoptotic, proliferative state. Both intermediate and nonclassical subsets were defined by cell differentiation genes. The nonclassical subset was defined by categories that indicate a proapoptotic, antiproliferative state. *CDKN1C*, a potent cell-cycle inhibitor, was the third most highly expressed gene for the nonclassical subset (Table 3). These show that the nonclassical subset is the most mature subset, as cell-cycle withdrawal is normally associated with highly differentiated cells.[28] The results of this analysis were consistent with previous studies, which show that the $CD16^+$ monocytes were proapoptotic[29] and that $CD16^+$ monocytes are more mature.[19,30]

The 3 monocytes subsets are defined by different transcriptional profiles

Transcription factors are key regulators of gene expression. We list the transcription factors found among the 1554 differentially

Table 2. Top 50 genes most highly expressed by the intermediate monocyte subset sorted according to decreasing absolute fold change values

	Fold change normalized to intermediate*	
Gene name	**Classic**	**Nonclassic**
GDNF family receptor-α2 (GFRA2)	−5.25	−2.62
Natural killer cell group 7 sequence (NKG7)	−4.86	−1.03
Plasmalemma vesicle associated protein (PLVAP)	−4.53	−1.28
Placenta-specific 8 (PLAC8)	−3.35	−1.33
MARCKS-like 1 (MARCKSL1)	−3.23	−1.01
E2F transcription factor 2 (E2F2)	−3.05	−1.22
Quanylate binding protein 4 (GBP4)	−3.03	−1.00
C-type lectin domain family 10 member A (CLEC10A)	−1.48	−2.73
Complement component 1 q subcomponent C chain (C1QC)	−2.72	−1.10
Epithelial V-like antigen 1 (EVA1)	−1.07	−2.67
c-mer proto-oncogene tyrosine kinase (MERTK)	−2.65	−1.04
Monoglyceride lipase (MGLL)	−2.59	−1.06
Development and differentiation enhancing factor-like 1 (DDEFL1)	−2.47	−1.00
Macrophage receptor with collagenous structure (MARCO)	−1.68	−2.44
Nuclear receptor subfamily 1 group H member 3 (NR1H3)	−2.41	−1.57
Fructose-16-bisphosphatase 1 (FBP1)	−2.39	−1.36
Acid phosphatase 2 lysosomal (ACP2)	−2.36	−1.08
Guanylate binding protein 1 interferon-inducible 67kDa (GBP1)	−2.27	−1.26
G protein-coupled bile acid receptor 1 (GPBAR1)	−2.24	−1.20
SAM and SH3 domain containing 1 (SASH1)	−2.24	−1.36
Olfactomedin 1 (OLFM1)	−1.21	−2.20
TIMP metallopeptidase inhibitor 1 (TIMP1)	−2.17	−1.08
Major histocompatibility complex class II DO-α (HLA-DOA)	−1.74	−2.15
Calcium/calmodulin-dependent protein kinase I (CAMK1)	−2.14	−1.04
Protein O-fucosyltransferase 1 (POFUT1)	−2.13	−1.02
Erythrocyte membrane protein band 4.1-like 3 (EPB41L3)	−2.09	−1.21
H19 imprinted maternally expressed untranslated mRNA (H19)	−2.08	−2.11
Stearoyl-CoA desaturase (SCD)	−1.69	−2.04
Coactosin-like 1 (COTL1)	−2.03	−1.07
Solute carrier family 29 member 1 (SLC29A1)	−2.02	−1.02
DNA-damage-inducible transcript 4 (DDIT4)	−1.14	−2.01
Transglutaminase 2 (TGM2)	−2.00	−1.67
Leukocyte immunoglobulin-like receptor subfamily A member 3 (LILRA3)	−1.99	−1.00
Activating transcription factor 5 (ATF5)	−1.48	−1.99
Glycoprotein A33 (GPA33)	−1.98	−1.04
Zinc finger protein 703 (ZNF703)	−1.98	−1.05
Sorting nexin 5 (SNX5)	−1.96	−1.01
C-type lectin domain family 10 member A (CLEC10A)	−1.37	−1.96
Tubulin-α ubiquitous (K-ALPHA-1)	−1.92	−1.17
Major histocompatibility complex class II DP-β 1 (HLA-DPB1)	−1.46	−1.91
Dehydrogenase/reductase member 9 (DHRS9)	−1.41	−1.90
Methylenetetrahydrofolate dehydrogenase 2 (MTHFD2)	−1.89	−1.21
ral guanine nucleotide dissociation stimulator-like 1 (RGL1)	−1.89	−1.51
PR domain containing 1 with ZNF domain (PRDM1)	−1.04	−1.89
Fatty acid desaturase 1 (FADS1)	−1.05	−1.88
Solute carrier family 2 member 8 (SLC2A8)	−1.87	−1.22
c-src tyrosine kinase (CSK)	−1.86	−1.08
Isochorismatase domain containing 2 (ISOC2)	−1.82	−1.10
CD300c antigen (CD300C)	−1.81	−1.19
FYVE RhoGEF and PH domain containing 2 (FGD2)	−1.78	−1.04

*Obtained by calculating the MFI values of classical or nonclassical relative to intermediate.

expressed genes sorted according to highest expression by classical (Figure 4A), intermediate (Figure 4B), and nonclassical (Figure 4C).

Transcriptional complexes consisting of interacting transcription factors activate, repress or direct gene transcription. We used Ingenuity Pathway Analysis to reveal the known protein-protein interactions within transcription factors most highly expressed by each monocyte subset. For classical monocytes, the interaction network was dominated by components of the AP-1 transcription factor (Figure 4D). These include JUN, FOS, ATF, and MAF family members that dimerize through leucine zippers motifs.[31] Different heterodimers of these components define the transcription targets for AP-1. In addition, positive (*DDIT3*) and negative (*BATF*) regulators of AP-1 were also present.[32,33] Hence, the ability of classical monocytes to respond to a diverse range of stimuli may at least in part be the result of the activity of different AP-1 components triggered by different stimuli and signaling pathways.

The interaction network for the nonclassical subset featured transcriptional activities involving control of differentiation, apoptosis, and proliferation (Figure 4E). These included *SPI1*, *MAF*, *ETS1*, and *CEBPA*. *CEBPA*, through its inhibitive interaction with

Table 3. Top 50 genes most highly expressed by the nonclassical monocyte subset sorted according to decreasing absolute fold change values

	Fold change normalized to intermediate*	
Gene name	**Classic**	**Nonclassic**
Complement component 1 q subcomponent-α polypeptide (C1QA)	−15.64	1.47
Hairy and enhancer of split 4 (HES4)	−14.80	1.58
Cyclin-dependent kinase inhibitor 1C (CDKN1C)	−14.06	1.62
Complement component 1 q subcomponent-β polypeptide (C1QB)	−11.56	1.36
ras homolog gene family member C (RHOC)	−8.63	1.25
C-type lectin domain family 4 member F (CLEC4F)	−8.32	1.43
Adenosine deaminase (ADA)	−7.05	1.63
Transgelin (TAGLN)	−6.06	1.60
Transcription factor 7-like 2 (TCF7L2)	−5.96	1.28
CD79B antigen (CD79B)	−5.83	1.77
Cathepsin L (CTSL)	−5.28	1.31
Surfactant pulmonary-associated protein D (SFTPD)	−4.74	2.07
ABI gene family member 3 (ABI3)	−4.65	1.08
SET binding protein 1 (SETBP1)	−4.61	1.47
Fibroblast growth factor receptor-like 1 (FGFRL1)	−4.54	1.19
CD79B antigen (CD79B)	−4.31	1.48
Sprouty-related EVH1 domain containing 1 (SPRED1)	−4.23	1.19
Jun dimerization protein p21SNFT (SNFT)	−4.23	1.35
Enah/Vasp-like (EVL)	−4.21	1.12
Metastasis suppressor 1 (MTSS1)	−4.00	1.72
SH2 domain containing 1B (SH2D1B)	−2.38	3.79
Cytoplasmic FMR1 interacting protein 2 (CYFIP2)	−3.94	1.42
Nasal embryonic LHRH factor (NELF)	−3.92	1.06
Cbl-interacting protein Sts-1 (STS-1)	−3.83	1.18
Sialic acid binding Ig-like lectin 10 (SIGLEC10)	−3.63	1.46
CDC28 protein kinase regulatory subunit 1B (CKS1B)	−3.63	1.23
Protein tyrosine phosphatase type IVA member 3 (PTP4A3)	−3.61	1.97
LY6/PLAUR domain containing 2 (LYPD2)	−3.59	5.87
SID1 transmembrane family member 2 (SIDT2)	−3.59	1.26
Insulin-induced gene 1 (INSIG1)	−3.59	1.61
Lymphotoxin-β (LTB)	−3.50	1.27
3′-Phosphoadenosine 5′-phosphosulfate synthase 2 (PAPSS2)	−3.41	1.38
ATP-binding cassette subfamily C member 3 (ABCC3)	−3.41	1.79
Caspase 5 apoptosis-related cysteine peptidase (CASP5)	−3.39	1.65
Vitelline membrane outer layer 1 homolog (chicken; VMO1)	−1.35	3.28
Heat shock 27kDa protein 1 (HSPB1)	−3.27	1.09
Guanine nucleotide binding protein-γ transducing activity polypeptide 2 (GNGT2)	−3.26	1.16
Heme oxygenase (decycling) 1 (HMOX1)	−3.25	1.34
Related RAS viral (r-ras) oncogene homolog (RRAS)	−3.22	1.21
Ring finger protein 122 (RNF122)	−3.21	1.59
Cadherin-like 23 (CDH23)	−3.20	3.60
Formin-like 2 (FMNL2)	−3.20	1.60
Regulator of G-protein signalling 12 (RGS12)	−3.19	1.29
Secretoglobin family 3A member 1 (SCGB3A1)	−3.17	2.07
fer-1-like 3 myoferlin (C. elegans) (FER1L3)	−3.15	1.11
Calmodulin-like 4 (CALML4)	−3.08	1.12
Interferon-induced transmembrane protein 3 (IFITM3)	−3.07	1.03
Creatine kinase brain (CKB)	−2.22	3.07
Interferon-induced transmembrane protein 1 (IFITM1)	−3.04	1.30
Carcinoembryonic antigen-related cell adhesion molecule 3 (CEACAM3)	−2.99	1.22

*Obtained by calculating the MFI values of classical or nonclassical relative to intermediate.

E2F1, is strongly antiproliferative.[34] A stable, mutual antagonism of *CEBPA* and *SPI1* has been proposed to be important for permanent lineage commitment.[35] *CEBPA* interaction activates *FOXO1*, which results in cell-cycle arrest and apoptosis.[36] The association of *MAF* with *ETS1* renders cells refractory to proliferative signals from *CSF1R*.[37] Overall, this network reflects the antiproliferative, proapoptotic, and highly differentiated state of nonclassical monocytes.

There were also 4 transcription factor interaction pairs observed for the nonclassical monocytes, of which 3, namely, *HDAC6* with *CBFA2T3, MBD2* with *RBBP7*, and *PCGF2* with *RYBP*, function as transcriptional repressors. Another transcriptional repressor, HES4 is one of the second most highly expressed genes for nonclassical monocytes (Table 3). Similarly, GO analysis had revealed enrichment in categories involved in negative regulation of transcription (supplemental Table 4). Hence, the nonclassical subset is also defined by several transcriptional repression activities.

The 7 transcription factors most highly expressed by the intermediate monocytes were not predicted to form direct interactions. Given

Table 4. GO enrichment analysis of biologic processes related to the maturation state of the 3 monocyte subsets

Term	Count	%	*P*
Classical monocyte subset			
Apoptosis			
GO:0006916: antiapoptosis	27	3.52	5.32E-06
GO:0043066: negative regulation of apoptosis	35	4.56	7.91E-05
GO:0042981: regulation of apoptosis	61	7.94	3.39E-04
GO:0006915: apoptosis	43	5.60	8.33E-03
Proliferation			
GO:0008284: positive regulation of cell proliferation	34	4.43	2.64E-03
GO:0042127: regulation of cell proliferation	55	7.16	4.12E-03
GO:0008283: cell proliferation	34	4.43	5.77E-03
GO:0008285: negative regulation of cell proliferation	26	3.39	3.91E-02
Intermediate monocyte subset			
Apoptosis			
GO:0042981: regulation of apoptosis	12	10.26	3.28E-02
GO:0008624: induction of apoptosis by extracellular signals	4	3.42	4.89E-02
Cell differentiation			
GO:0045596: negative regulation of cell differentiation	7	5.98	5.05E-03
Nonclassical monocyte subset			
Apoptosis			
GO:0042981: regulation of apoptosis	51	10.32	4.91E-06
GO:0006917: induction of apoptosis	26	5.26	3.58E-05
GO:0043065: positive regulation of apoptosis	31	6.28	5.31E-05
GO:0008624: induction of apoptosis by extracellular signals	14	2.83	6.20E-05
GO:0006915: apoptosis	35	7.09	8.86E-04
GO:0043066: negative regulation of apoptosis	21	4.25	1.07E-02
GO:0006916: antiapoptosis	13	2.63	3.48E-02
Proliferation			
GO:0042127: regulation of cell proliferation	50	10.12	5.75E-06
GO:0008285: negative regulation of cell proliferation	25	5.06	6.17E-04
GO:0008284: positive regulation of cell proliferation	24	4.86	7.38E-03
Cell differentiation			
GO:0045637: regulation of myeloid cell differentiation	7	1.42	2.49E-02
GO:0002521: leukocyte differentiation	10	2.02	2.56E-02
GO:0030098: lymphocyte differentiation	8	1.62	4.83E-02

the close relationship between intermediate and nonclassical subsets, we explored whether the transcription factors of the intermediate subset could interact and/or increase the expression of transcription factors most highly expressed by the nonclassical subset (Figure 4F). This revealed reciprocal increases in the transcription factor genes found in both subsets. Direct interactions were also found. Notably, several of these transcription factors, including *SPI1*, *NCOA3*, *CEBPA*, *E2F1*, and *CCNE1*, were found within the main network of transcription factors in the nonclassical subset (Figure 4E). This indicates a possible continuum of transcription factor activity between the intermediate and nonclassical subsets.

The 3 monocyte subsets possess different repertoires of cell surface receptor genes

Next, we highlighted surface receptor genes among the 1554 differentially expressed genes (supplemental Figure 1). These represent potential surface markers that can be used to distinguish between the monocyte subsets. We categorized these receptors into scavenger and lipoprotein receptors, carbohydrate binding receptors, adhesion receptors, chemokine receptors, cytokine receptors, and G-protein coupled receptors (GPCR). We observed that the majority of scavenger/low density lipoprotein receptors and carbohydrate binding receptor genes were most highly expressed by the classic monocyte subset. Together, these receptors are responsible for recognition and uptake of a diverse array of self and pathogenic ligands.[38,39] This reinforces the GO analysis results, which show that classical monocytes were highly versatile and responsive to a large variety of external cues. The classical and nonclassical monocyte subsets express a different array of chemokine receptors, adhesion receptors, cytokine receptors, and GPCRs. The intermediate subset most highly expressed a small number of receptor genes, including *MARCO*, *CLEC10A*, *CMKLR1*, *GFRA2*, *IFNAR2*, *GPR30*, *GPR35*, *GPBAR1*, *CD40*, and *CD300C*.

Flow cytometric analysis of surface markers by the 3 monocyte subsets

We next wanted to identify unique surface markers that could be used to distinguish the 3 monocyte subsets by flow cytometry. First, a panel of established surface markers previously described for monocyte subsets was tested. In Figure 5A, representative histogram plots for each tested marker are shown. In Figure 5B, the mean ± SD of the median fluorescence intensity (MFI) subtracted by the fluorescence minus one (FMO) isotype control are shown. Statistically significant differences between the monocyte subsets are also indicated. We found that several markers, including CD64, CCR1, CCR2, CX_3CR1, CD11b, CD33, and CD115, were expressed at the intermediary level for the intermediate monocyte subset. CD40, CD54, and HLA-DR were most highly expressed by the intermediate subset. CXCR1, CXCR2, and CD62L were expressed almost only by the classical monocytes. SLAN was expressed by a subset of nonclassical monocytes.

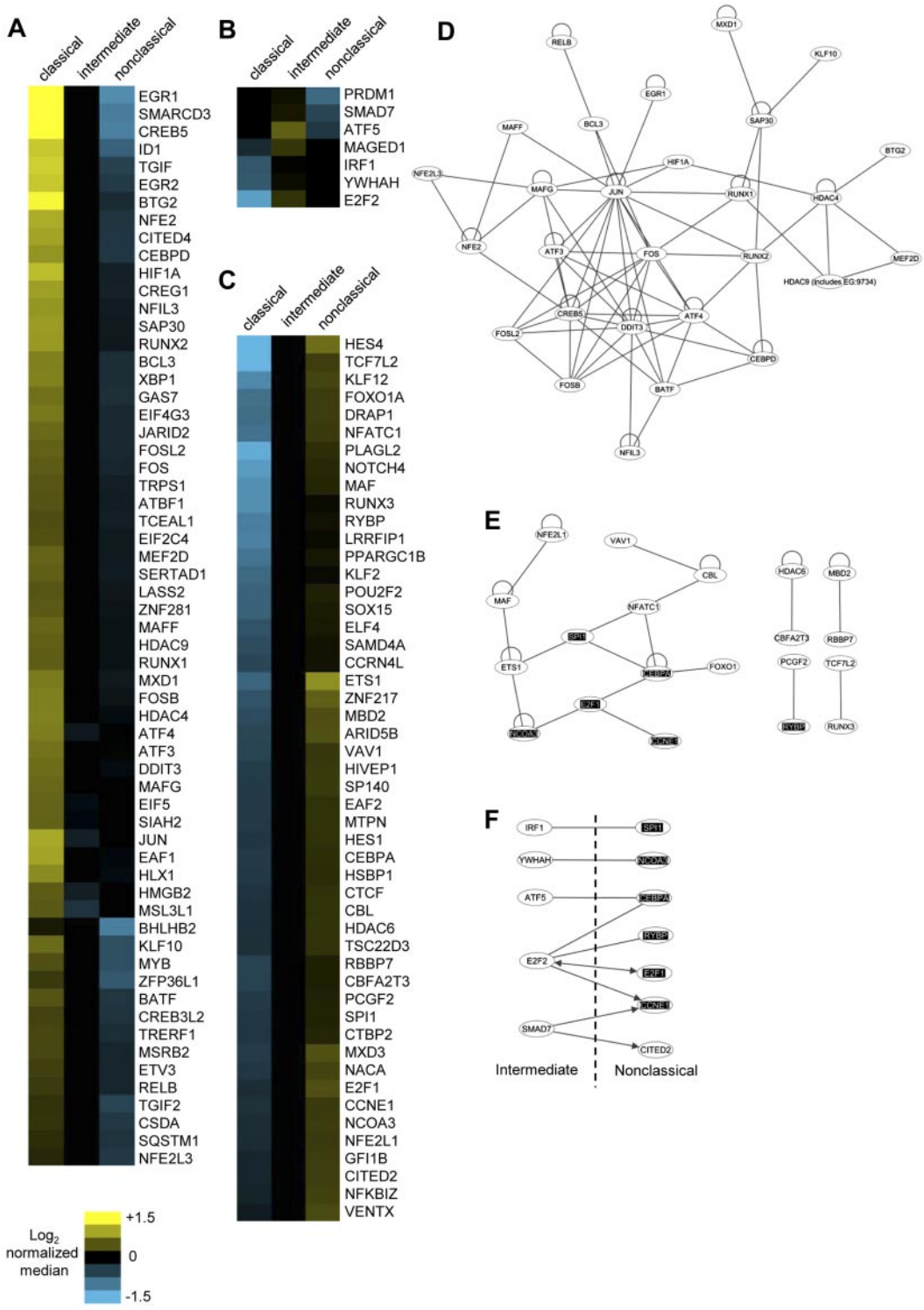

Figure 4. Transcription factor genes most highly expressed by each monocyte subset and the analysis of their protein-protein interactions. Transcription factors most highly expressed by (A) classical, (B) intermediate, and (C) nonclassical subsets are shown. The normalized $\log_2$ MFIs for each gene are illustrated in corresponding heat maps. Possible known direct protein-protein interactions between the transcription factors most highly expressed by the (D) classical, (E) nonclassical, and (F) the intermediate plus nonclassical subset combined were revealed using Ingenuity Pathway Analysis. Common transcription factor genes found in panels E and F are highlighted. Lines represent direct protein-protein interactions; loops, homodimerization; and arrows, direct increase in expression.

We next performed flow cytometry on a selected list of novel surface markers identified by microarray (supplemental Figure 1). These markers were grouped based on the monocyte subset that showed highest expression for these markers in microarray (Figure 6). Flow cytometric results reveal that classical monocytes expressed the highest surface protein levels of CD1d, CD9, CD36, CD99, CD163, and CLEC5A (Figure 6A). The intermediate subset expressed these markers at an intermediary level between the classical and nonclassic subset. CLEC4D and IL-13Rα1 surface expression was detected only for the classical subset. We found that

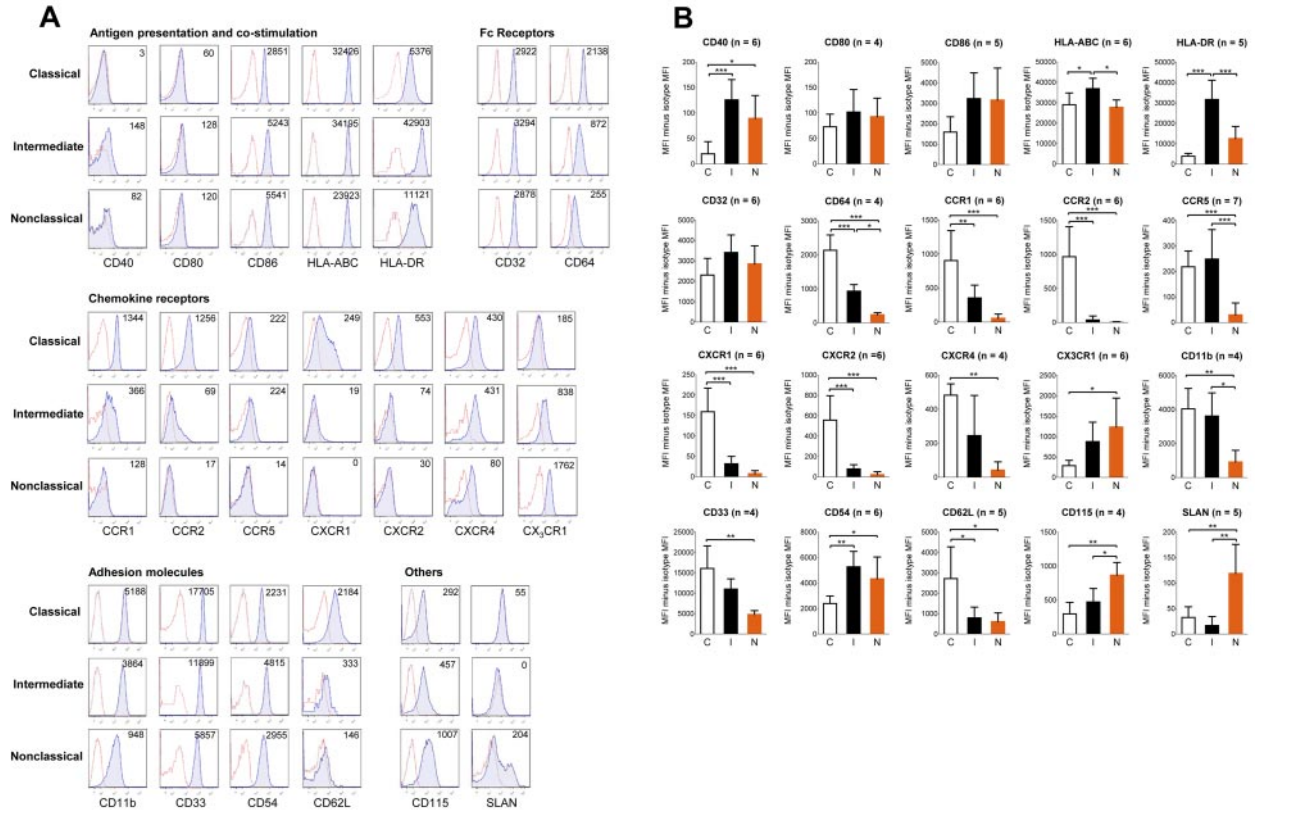

Figure 5. Flow cytometric analysis of established monocyte surface markers. (A) After doublet and dead cell exclusion with 7-aminoactinomycin D, gating on the 3 monocyte subsets for both specific and background staining was done based on CD14 and CD16 expression as shown in Figure 1A. Specific stainings are represented by blue tinted histograms, whereas FMO isotype controls are represented by histograms with red dotted lines. Numbers in each histogram represent MFI of specific staining minus isotype control. Representative data from 4 to 7 independent donors. (B) The mean ± SD of the MFI of the specific staining minus the MFI of its FMO isotype control for the tested surface antigens are shown. The number of persons the results for each surface marker is based on is denoted by (n). Statistical calculations of significance were performed using ANOVA followed by post-hoc Tukey for significant differences between any 2 monocyte subsets: $*P < .05$, $**P < .01$, $***P < .001$.

GFRα2 and CLEC10A were lowly, but consistently and specifically, expressed by the intermediate monocyte subset (Figure 6B). Nonclassical monocytes expressed the highest levels of CD97, CD123, P2RX1, and Siglec10, whereas the intermediate monocytes expressed these markers at relative lower levels (Figure 6C). The expression of CD294 was low but specifically expressed by the nonclassical monocyte subset. In Figure 6D, we show the mean ± SD minus FMO isotype control for each surface marker, and the differences that are statistically significant between the monocyte subsets.

We have provided a summary of the surface markers that can uniquely separate the 3 monocyte subsets (Table 5). This table lists surface markers that are statistically significant for at least 2 comparison between the 3 monocyte subsets (classical vs intermediate, classical vs nonclassical, intermediate vs nonclassical), and the respective fold changes values, calculated based on average MFI between any 2 subsets. Surface markers that are statistically significantly different between 2 comparisons uniquely separate a particular subset. For example, the expression of CLEC4D is significantly different between the classical versus intermediate and classical versus nonclassical subset, but not between the intermediate versus nonclassical monoyctes. CLEC4D can hence be used to uniquely separate the classical subset from the other 2 subsets. These markers were ordered according to increasing statistical significance for each monocyte subset.

If monocyte subsets represent a single lineage at different stages of maturation, then gradual changes in the surface expression of markers would be observed. We analyzed the expression of several surface markers based on increasing CD16 and decreasing CD14 expression as depicted in Figure 6E. Specifically, classical monocytes were represented by a single R1 gate, whereas the intermediate monocytes was subdivided into 3 gates (R2, R3, and R4) based on increasing in CD16 expression. The nonclassical subset was subdivided into 3 gates (R5, R6, and R7) based on decreasing in CD14 expression. As we followed the expression of representative markers from R1 to R7 gates, we observed the gradual decrease in expression of several markers that were most highly expressed by the classical subset. Likewise, a gradual increase was observed with several markers mostly highly expressed by the nonclassical subset. This pattern of surface marker expression provides circumstantial support for the continuum of maturation stages by the monocyte subsets.

Distinct cytokine production patterns revealed by LPS activation

Lastly, we compared the cytokine production of the monocyte subsets after activation (Figure 7). Consistently through increasing doses of LPS, the classical monocytes produced the highest levels of the broadest range of cytokines, including granulocyte colony-stimulating factor, IL-10, CCL2, regulated on activation normal T expressed and secreted, and IL-6. In our hands, the nonclassical subset produced the highest levels of the inflammatory cytokines, TNF-α, and IL-1β. For the intermediate subset, the levels of these cytokines and chemokines were produced at either the lowest or intermediary level.

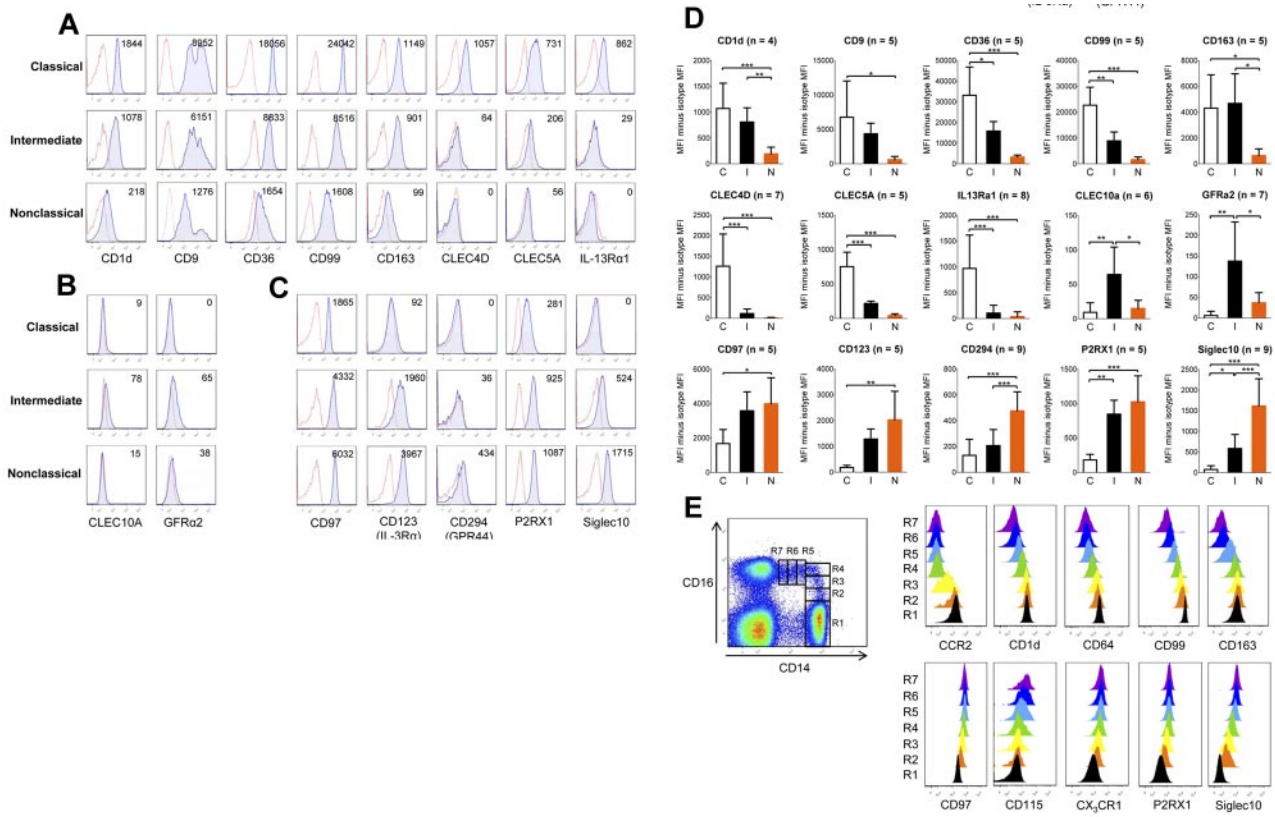

Figure 6. Flow cytometric analysis of novel surface markers identified by microarray. After doublet and dead cell exclusion with 7-aminoactinomycin D, gating on the 3 monocyte subsets for both specific and background staining was done based on CD14 and CD16 expression as shown in Figure 1A. Specific stainings are represented by blue tinted histograms, whereas FMO isotype controls are represented by histograms with red dotted lines. Surface markers were categorized according to the monocyte subset showing highest expression in microarray: (A) classical, (B) intermediate, and (C) nonclassical. Numbers in each histogram represent MFI of specific staining minus isotype control. (D) The mean ± SD of the MFI of the specific staining minus the MFI of its FMO isotype control for the surface antigens. n represents the number of persons on which the results for each surface marker is based. Statistical calculations of significance were performed using ANOVA followed by the post-hoc Tukey test for significant differences between any 2 monocyte subsets: $*P < .05$, $**P < .01$, $***P < .001$. (E) The expression of representative markers was tracked based on increasing CD16 and decreasing CD14 expression. The intermediate monocyte subset was further subdivided based on increasing CD16 expression using R2, R3, and R4 gates. The nonclassical monocyte subset was further subdivided based on decreasing CD14 expression using R5, R6, and R7 gates. The classical subset was identified by R1 gate. Colored plots representing histograms from R1 to R7 were created using FlowJo software.

Discussion

The new official nomenclature for monocyte subsets presents new challenges to the field of monocyte heterogeneity, as $CD16^+$ monocytes are now no longer considered to be homogeneous. Our study provides a comprehensive definition of the 3 circulating monocyte subsets, through which the close relationship between the human intermediate and nonclassical monocyte subsets was revealed. This result is different from the study by Cros et al[9] but consistent with the relationship described for the 3 homologous monocyte subsets of macaque monkeys that was also identified using CD14 and CD16 expression.[22] Our results, together with other recent genome-wide analysis of human monocyte subsets,[9,19,21,40,41] provide a comprehensive definition for the monocyte subsets during healthy conditions. This serves as the basis for the identification of targets that may be altered during disease conditions, particularly diseases associated with monocytosis and/or alterations in the proportion of monocyte subsets.

Although the intermediate and nonclassical monocytes are very closely related, there were also features to distinguish them apart. One example is MHC class II expression, which was highest with the intermediate monocyte subset. The high MHC class II expression indicates that intermediate monocytes may possess superior T-cell stimulatory functions. Indeed, this was demonstrated with $CD16^+CD64^+$ monocytes, a phenotype that matches with the intermediate subset.[14] Based on our microarray results, the nonclassical subset most highly expressed several genes involved in cytoskeleton rearrangement. This may represent the molecular basis of their highly motile, "patrolling" behavior observed in vivo,[9] and other predicted abilities, such as FcR-mediated phagocytosis.

Another distinguishing feature of the nonclassical subset was the high levels of TNF-α and IL-1β produced in response to LPS. This result was consistent with a previous study by Belge et al.[20] In that study, TNF-α was detected using intracellular staining in whole blood after activation with Toll-like receptor ligands. Their method involves very little in vitro manipulation, avoiding issues of nonspecific activation through isolation and culture. Indeed, discrepant results on cytokine production by isolated monocyte subsets after LPS stimulation has been reported.[9,10] One possible reason for this discrepancy is the use of different anti-CD14 antibody clones for cell sorting of the monocyte subsets. Certain anti-CD14 clones, such as M5E2, are known to block LPS activity.[42] Monocytes isolated using such anti-CD14 clones may exhibit diminished responses to LPS. The anti-CD14 clone used in this study (61D3) is not known to exhibit any LPS inhibitory activity.[43] Therefore, our results and the results of others[20] demonstrate the preferential ability of the nonclassical monocyte subset to produce higher levels of TNF-α and IL-1β in response to LPS. This

Table 5. Systematic summary of surface markers that uniquely separates the 3 monocyte subsets

	MFI minus isotype MFI (mean ± SD)			Average fold change			*P*		
Marker	**Classical**	**Intermediate**	**Nonclassical**	**C vs I**	**C vs N**	**I vs N**	**C vs I**	**C vs N**	**I vs N**
Classical monocyte subset									
CD62L (n = 5)	2715 ± 1555	790 ± 527	605 ± 426	3.4	4.5	1.3	*	*	NS
CD54 (n = 6)	2385 + 588	5270 ± 1207	4326 ± 1717	−2.2	−1.8	1.2	†	*	NS
CD40 (n = 6)	20 ± 24	126 ± 40	90 ± 45	−6.4	−4.5	1.4	‡	*	NS
CD36 (n = 5)	33 184 ± 13 648	15 853 ± 4591	3244 ± 950	2.1	10.2	4.9	*	‡	NS
CD99 (n = 5)	22 692 ± 6961	8914 ± 3415	1594 ± 1074	2.5	14.2	5.6	†	‡	NS
CCR1 (n = 6)	905 ± 440	355 ± 188	55 ± 63	2.6	16.4	6.4	†	‡	NS
P2XR1 (n = 5)	182 ± 82	847 ± 202	1026 ± 378	−4.7	−5.6	−1.2	†	‡	NS
CCR2 (n = 6)	968 ± 440	36 ± 59	4 ± 7	26.7	230.5	8.6	‡	‡	NS
CLEC4D (n = 7)	1260 ± 778	115 ± 110	6 ± 15	11.0	200.1	18.2	‡	‡	NS
CLEC5A (n = 5)	753 ± 209	217 ± 34	43 ± 23	3.5	17.4	5.0	‡	‡	NS
CXCR1 (n = 6)	159 ± 58	32 ± 18	7 ± 8	5.0	21.5	4.3	‡	‡	NS
CXCR2 (n = 6)	557 ± 239	78 ± 42	23 ± 28	7.1	24.6	3.4	‡	‡	NS
IL13Ra1 (n = 8)	971 ± 647	107 ± 151	39 ± 92	9.1	24.6	2.7	‡	‡	NS
CD64 (n = 4)	2135 ± 449	931 ± 193	236 ± 58	2.3	9.0	3.9	‡	‡	*
Intermediate monocyte subset									
HLA-ABC (n = 6)	29 026 + 5768	36 894 + 5088	27 796 + 3563	−1.3	1.0	1.3	*	NS	*
CLEC10A (n = 6)	9 ± 14	64 ± 40	15 ± 12	−6.9	−1.6	4.3	†	NS	*
GFRA2 (n = 7)	6 ± 10	138 ± 95	37 ± 25	−6.2	−23.0	3.7	†	NS	*
HLA-DR (n = 5)	3916 ± 1363	31 755 ± 9410	12 584 ± 5924	−8.1	−3.2	2.5	‡	NS	†
Nonclassical monocyte subset									
CD163 (n = 5)	4310 ± 2587	4678 ± 2295	632 ± 526	−1.1	6.8	7.4	NS	*	*
CD115 (n = 4)	295 ± 170	470 ± 199	865 ± 187	−1.6	−2.9	−1.8	NS	†	*
CD11b (n = 4)	4043 ± 1197	3617 ± 1365	915 ± 684	1.1	4.4	4.0	NS	†	*
SLAN (n = 5)	32.4 ± 21.0	16.8 ± 17.5	119.0 ± 56.9	1.9	−3.7	−7.1	NS	†	†
CD1d (n = 4)	1072 ± 528	810 ± 297	193 ± 138	1.3	5.5	4.2	NS	‡	†
CCR5 (n = 7)	219 ± 62	249 ± 116	30 ± 47	−1.1	7.3	8.3	NS	‡	‡
CD294 (n = 9)	131 ± 124	207 ± 124	476 ± 147	−1.6	−3.6	−2.3	NS	‡	‡
Siglec10 (n = 9)	76 ± 92	584 ± 340	1615 ± 659	−7.7	−21.3	−2.8	*	‡	‡

C indicates classical monocyte subset; I, intermediate monocyte subset; N, nonclassical monocyte subset; n, the number of individuals tested for each surface marker; and NS, not significant.

*$P < .05$ (ANOVA and post-hoc Tukey test).

†$P < .01$ (ANOVA and post-hoc Tukey test).

‡$P < .001$ (ANOVA and post-hoc Tukey test).

does not support the notion that the nonclassical subets respond selectively to viruses and damaged cells.[9]

We additionally describe new defining features for the classical monocyte subset. According to microarray results, classical monocytes expressed the broadest range of sensing receptor genes, and also genes involved in a wide diversity of functions, including tissue repair and immune responses. Furthermore, the relatively high expression of proinflammatory *S100A12* and *S100A8/9* genes[25] may underlie the ability of classical monocytes to support inflammation. In addition, classical monocytes produced high levels of the broadest range of cytokines and chemokines in response to LPS. We propose that this versatility of classical monocytes is attributed to AP-1 transcriptional factors that are most highly expressed at the gene level by classical monocytes. Different combinations of the AP-1 transcription factor components are activated by different stimuli and signaling pathways, defining the transcription targets for AP-1.[31-33] Nevertheless, these observations were made with microarray results and may not translate into actual protein expression that is quantitatively similar to differences in mRNA levels, therefore requiring further confirmation.

We analyzed surface markers for their usefulness for separating the 3 monocyte subsets (Table 5). Several markers, CCR2, CXCR1, CXCR2, CLEC4D, and IL-13Rα1, were found to be expressed almost solely by the classical monocyte subset. For the intermediate subset, HLA-ABC, HLA-DR, and CD40 were expressed at significantly higher levels. Furthermore, GFRα2 and CLEC10A were lowly, but almost exclusively, expressed by the intermediate subset. Given the close relationship between the intermediate and nonclassical subset, it may be difficult to identify surface markers that clearly segregate these 2 subsets. For example, the expression of CD115, CX_3CR1, CD97, CD123, P2RX1, and Siglec10 was shared. However, CD115, CD294, and Siglec10 were expressed at significantly higher levels for the nonclassical subset. Furthermore, several markers, including CCR5, CD11b, CD1d, and CD163, were significantly higher for the intermediate subset. Hence, using a combination of such markers could provide a clear separation between the intermediate and nonclassical monocyte subsets.

An important question is whether monocyte subsets represent distinct endpoints of differentiation or a single lineage at different stages of differentiation. The intermediate subset has been proposed to represent the direct intermediary link between the classical and nonclassical monocyte subsets.[16,18] Our results provide circumstantial evidence to support this notion. We observed a large majority of genes and surface markers expressed at an intermediary level between the classical and nonclassical subset. The intermediate monocyte subset did not possess inherent specialties in cytokine production, and there are gradual changes in surface marker expression for the monocyte subsets. Our microarray results also indicate an increase in maturation status from the classical, intermediate, to nonclassical subset.

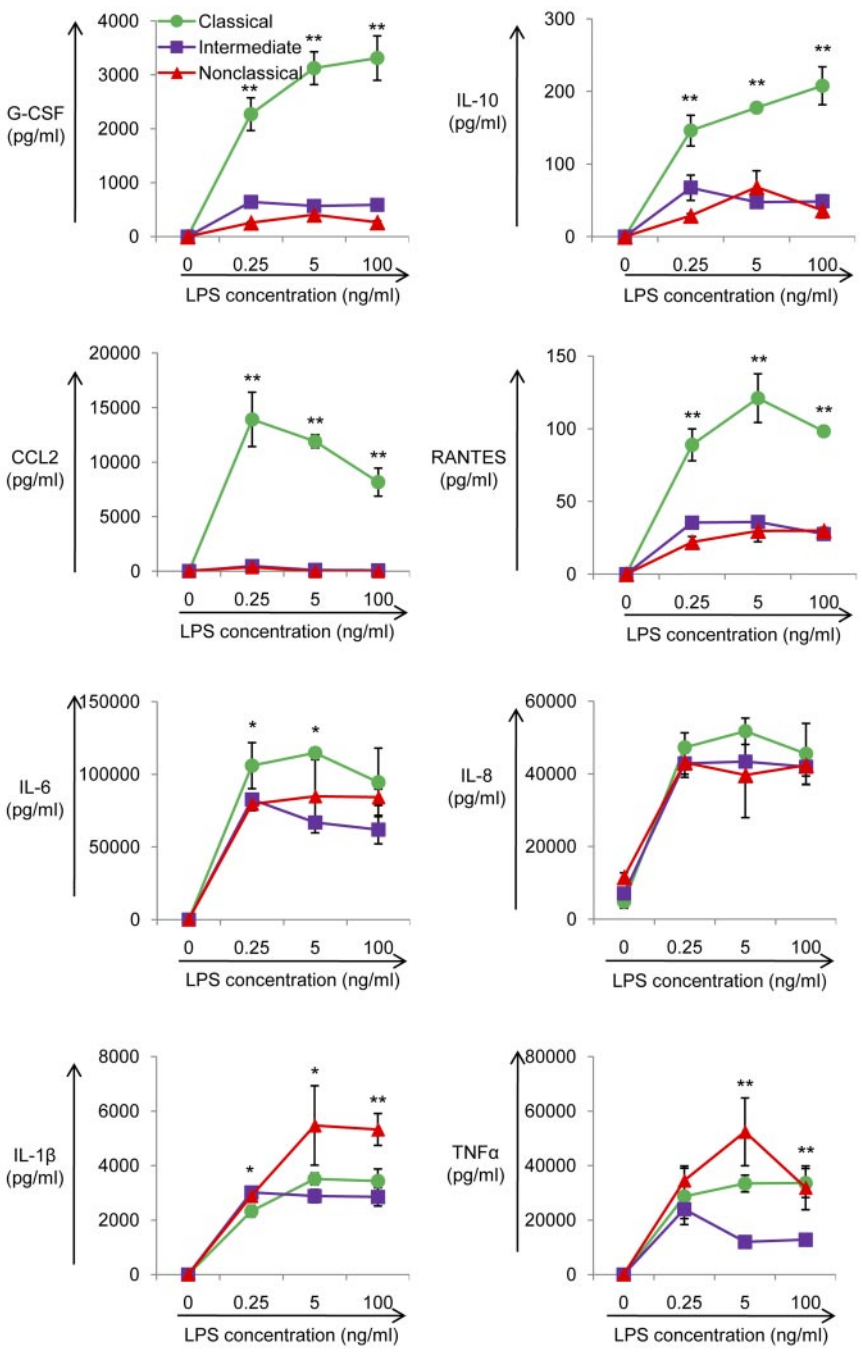

Figure 7. Differential cytokine production by the 3 monocyte subsets after activation with LPS. Purified monocyte subsets were treated with increasing doses of LPS. After 18 hours of culture, supernatants were harvested and cytokines and chemokines produced by the classical (●), intermediate (■), and nonclassical (▲) were measured using Bio-Plex human cytokine assay kits. Data are shown as mean ± SD. Representative data are from 4 experiments. *$P < .05$ (ANOVA). **$P < .005$ (ANOVA).

With preliminary in vitro experiments, we find that classical monocytes spontaneously down-regulated several classical subset-associated markers, coupled with the acquisition of some, but not all, of the nonclassical subset-associated markers (data not shown). These in vitro experiments were not entirely conclusive, and formal proof of the lineage relationship between the 3 subsets is still required. One major limitation of these in vitro experiments is its inability to properly mimic differentiation conditions in vivo, by which the location, factors, and mechanisms involved are as yet unknown. Nevertheless, although our results do not directly prove the direct lineage relationship between the subsets, it does provide evidence at the molecular level that the intermediate monocyte subset indeed lay between the classical and nonclassical monocyte subset in terms of global gene expression and a wide panel of surface markers.

Our results have several important implications in clinical settings. Flow cytometry is an important clinical tool for objectively accessing hematologic malignancies, whereby abnormal cells are identified through the aberrant expression of surface markers.[44] Our results will be most relevant to identifying abnormalities in myeloid neoplasms with associated monocytosis. These include chronic myelomonocytic leukemia, juvenile myelomonocytic leukemia, acute myelomonocytic leukemia, and acute monocytic leukemia. For example, it was shown that surface markers are useful to distinguish between these different forms of myeloid neoplasms[45,46] and between chronic myelomonocytic leukemia,

myelodysplastic syndromes, and reactive monocytosis.[47,48] Recently, it was shown that immunosuppressive CD14$^+$HLA-DR$^{low/-}$ monocytes were present in B-cell non-Hodgkin lymphoma,[49] suggesting that monocytes can also play important roles in lymphoid neoplasms. However, studies on hematologic malignancies are thus far based on whole monocytes, much less is known about specific abnormalities pertaining to monocyte subsets. Analyzing abnormalities in monocyte subsets may lead to the identification of clinically useful targets for improved diagnosis, staging, classification, and prognosis of hematologic malignancies. As such, our results provide a wide panel of myeloid and monocyte-associated markers and their normal expression levels to study monocyte subsets in myeloid neoplasms associated with monocytosis.

CD16$^+$ monocytes are known to expand in infectious and inflammatory conditions (eg, sepsis and HIV).[6] However, understanding of the CD16$^+$ monocyte subsets with respect to mechanism of induction and contribution to disease is still unclear. Our results provide the basis for the detailed analysis of monocyte subsets in disease conditions by identifying targets that could be altered. This approach could identify new correlations and alterations to monocyte subsets with potential clinical utility and yield mechanistic insights into the phenomenon of elevated CD16$^+$ monocyte proportions in disease conditions.

Recent studies have highlighted the merit of subdividing the CD16$^+$ monocytes into the intermediate and nonclassical subsets. For example, severe asthma was associated with a preferential increase in the intermediate subset.[15] In HIV, the intermediate monocytes best support viral replication.[22,50] Hence, there may be preferential increase or involvement of the intermediate and nonclassical subsets under different disease conditions. Our results provide a definitive way to identify the intermediate and nonclassical monocyte subsets, which would be useful for such endeavors.

Acknowledgments

The authors thank the staffs of the flow cytometry and microarray units in the Biopolis Shared Facilities and the Singapore Immunology Network, Agency for Science, Technology and Research for their assistance in cell sorting and sample processing; Siew Min Ong and Jinmiao Chen for technical assistance; and all members of the P.K. laboratory, Veronique Angeli, Gwendalyn Randolph, Shuzhen Chong, Jean Pierre Abastado, and Muzlifah Haniffa for helpful discussions and critical reading of the manuscript.

This work was supported by the Biomedical Research Council, Agency for Science, Technology and Research, Singapore.

Authorship

Contribution: K.L.W. designed and performed research, collected, analyzed, and interpreted data, performed statistical analysis, and wrote the manuscript; J.J.-Y.T. and W.-H.Y. designed and performed research, collected and analyzed data, performed statistical analysis, and wrote the manuscript; W.-C.W. and H.H. contributed vital analytical tools, analyzed data, and performed statistical analysis; X.S. performed research and collected and analyzed data; P.K. designed research and contributed vital analytical tools; and S.-C.W. designed and performed research, analyzed and interpreted data, and wrote the manuscript.

Conflict-of-interest disclosure: The authors declare no competing financial interests.

Correspondence: Kok Loon Wong, Singapore Immunology Network, Agency for Science, Technology and Research, 8A Biomedical Grove, Level 4, Immunos, Singapore 138648; e-mail: wong_kok_loon@immunol.a-star.edu.sg.

References

1. Passlick B, Flieger D, Ziegler-Heitbrock HW. Identification and characterization of a novel monocyte subpopulation in human peripheral blood. *Blood.* 1989;74(7):2527-2534.
2. Gordon S, Taylor PR. Monocyte and macrophage heterogeneity. *Nat Rev Immunol.* 2005;5(12):953-964.
3. Frankenberger M, Sternsdorf T, Pechumer H, Pforte A, Ziegler-Heitbrock HW. Differential cytokine expression in human blood monocyte subpopulations: a polymerase chain reaction analysis. *Blood.* 1996;87(1):373-377.
4. Ancuta P, Rao R, Moses A, et al. Fractalkine preferentially mediates arrest and migration of CD16+ monocytes. *J Exp Med.* 2003;197(12):1701-1707.
5. Geissmann F, Jung S, Littman DR. Blood monocytes consist of two principal subsets with distinct migratory properties. *Immunity.* 2003;19(1):71-82.
6. Ziegler-Heitbrock L. The CD14+ CD16+ blood monocytes: their role in infection and inflammation. *J Leukoc Biol.* 2007;81(3):584-592.
7. Tacke F, Randolph GJ. Migratory fate and differentiation of blood monocyte subsets. *Immunobiology.* 2006;211(6):609-618.
8. Auffray C, Sieweke MH, Geissmann F. Blood monocytes: development, heterogeneity, and relationship with dendritic cells. *Annu Rev Immunol.* 2009;27:669-692.
9. Cros J, Cagnard N, Woollard K, et al. Human CD14dim monocytes patrol and sense nucleic acids and viruses via TLR7 and TLR8 receptors. *Immunity.* 2010;33(3):375-386.
10. Skrzeczynska-Moncznik J, Bzowska M, Loseke S, et al. Peripheral blood CD14high CD16+ monocytes are main producers of IL-10. *Scand J Immunol.* 2008;67(2):152-159.
11. Schakel K, Kannagi R, Kniep B, et al. 6-Sulfo LacNAc, a novel carbohydrate modification of PSGL-1, defines an inflammatory type of human dendritic cells. *Immunity.* 2002;17(3):289-301.
12. de Baey A, Mende I, Riethmueller G, Baeuerle PA. Phenotype and function of human dendritic cells derived from M-DC8(+) monocytes. *Eur J Immunol.* 2001;31(6):1646-1655.
13. Grage-Griebenow E, Flad HD, Ernst M. Heterogeneity of human peripheral blood monocyte subsets. *J Leukoc Biol.* 2001;69(1):11-20.
14. Grage-Griebenow E, Zawatzky R, Kahlert H, et al. Identification of a novel dendritic cell-like subset of CD64(+)/CD16(+) blood monocytes. *Eur J Immunol.* 2001;31(1):48-56.
15. Moniuszko M, Bodzenta-Lukaszyk A, Kowal K, Lenczewska D, Dabrowska M. Enhanced frequencies of CD14++CD16+, but not CD14+CD16+, peripheral blood monocytes in severe asthmatic patients. *Clin Immunol.* 2009;130(3):338-346.
16. Ziegler-Heitbrock L, Ancuta P, Crowe S, et al. Nomenclature of monocytes and dendritic cells in blood. *Blood.* 2010;116(16):e74-e80.
17. Ziegler-Heitbrock HW. Heterogeneity of human blood monocytes: the CD14+ CD16+ subpopulation. *Immunol Today.* 1996;17(9):424-428.
18. Weiner LM, Li W, Holmes M, et al. Phase I trial of recombinant macrophage colony-stimulating factor and recombinant gamma-interferon: toxicity, monocytosis, and clinical effects. *Cancer Res.* 1994;54(15):4084-4090.
19. Ancuta P, Liu KY, Misra V, et al. Transcriptional profiling reveals developmental relationship and distinct biological functions of CD16+ and CD16- monocytes. *BMC Genomics.* 2009;10:403.
20. Belge KU, Dayyani F, Horelt A, et al. The proinflammatory CD14+CD16+DR++ monocytes are a major source of TNF. *J Immunol.* 2002;168(7):3536-3542.
21. Ingersoll MA, Spanbroek R, Lottaz C, et al. Comparison of gene expression profiles between human and mouse monocyte subsets. *Blood.* 2010;115(3):e10-e19.
22. Kim WK, Sun Y, Do H, et al. Monocyte heterogeneity underlying phenotypic changes in monocytes according to SIV disease stage. *J Leukoc Biol.* 2010;87(4):557-567.
23. Wong WC, Loh M, Eisenhaber F. On the necessity of different statistical treatment for Illumina BeadChip and Affymetrix GeneChip data and its significance for biological interpretation. *Biol Direct.* 2008;3:23.
24. da Huang W, Sherman BT, Lempicki RA. Systematic and integrative analysis of large gene lists using DAVID bioinformatics resources. *Nat Protoc.* 2009;4(1):44-57.
25. Roth J, Vogl T, Sorg C, Sunderkotter C. Phagocyte-specific S100 proteins: a novel group of proinflammatory molecules. *Trends Immunol.* 2003;24(4):155-158.
26. Nobes CD, Hall A. Rho GTPases control polarity, protrusion, and adhesion during cell movement. *J Cell Biol.* 1999;144(6):1235-1244.
27. May RC, Machesky LM. Phagocytosis and the actin cytoskeleton. *J Cell Sci.* 2001;114(6):1061-1077.

28. Buttitta LA, Edgar BA. Mechanisms controlling cell cycle exit upon terminal differentiation. *Curr Opin Cell Biol.* 2007;19(6):697-704.
29. Zhao C, Tan YC, Wong WC, et al. The CD14(+/low)CD16(+) monocyte subset is more susceptible to spontaneous and oxidant-induced apoptosis than the CD14(+)CD16(−) subset. *Cell Death Dis.* 2010;1(11):e95.
30. Ziegler-Heitbrock HW, Fingerle G, Strobel M, et al. The novel subset of CD14+/CD16+ blood monocytes exhibits features of tissue macrophages. *Eur J Immunol.* 1993;23(9):2053-2058.
31. Chinenov Y, Kerppola TK. Close encounters of many kinds: Fos-Jun interactions that mediate transcription regulatory specificity. *Oncogene.* 2001;20(19):2438-2452.
32. Ubeda M, Vallejo M, Habener JF. CHOP enhancement of gene transcription by interactions with Jun/Fos AP-1 complex proteins. *Mol Cell Biol.* 1999;19(11):7589-7599.
33. Echlin DR, Tae HJ, Mitin N, Taparowsky EJ. B-ATF functions as a negative regulator of AP-1 mediated transcription and blocks cellular transformation by Ras and Fos. *Oncogene.* 2000; 19(14):1752-1763.
34. Johnson PF. Molecular stop signs: regulation of cell-cycle arrest by C/EBP transcription factors. *J Cell Sci.* 2005;118(12):2545-2555.
35. Laslo P, Spooner CJ, Warmflash A, et al. Multilineage transcriptional priming and determination of alternate hematopoietic cell fates. *Cell.* 2006; 126(4):755-766.
36. van der Horst A, Burgering BM. Stressing the role of FoxO proteins in lifespan and disease. *Nat Rev Mol Cell Biol.* 2007;8(6):440-450.
37. Klappacher GW, Lunyak VV, Sykes DB, et al. An induced Ets repressor complex regulates growth arrest during terminal macrophage differentiation. *Cell.* 2002;109(2):169-180.
38. Robinson MJ, Sancho D, Slack EC, LeibundGut-Landmann S, Reis e Sousa. Myeloid C-type lectins in innate immunity. *Nat Immunol.* 2006;7(12): 1258-1265.
39. Peiser L, Mukhopadhyay S, Gordon S. Scavenger receptors in innate immunity. *Curr Opin Immunol.* 2002;14(1):123-128.
40. Zhao C, Zhang H, Wong WC, et al. Identification of novel functional differences in monocyte subsets using proteomic and transcriptomic methods. *J Proteome Res.* 2009;8(8):4028-4038.
41. Mobley JL, Leininger M, Madore S, Baginski TJ, Renkiewicz R. Genetic evidence of a functional monocyte dichotomy. *Inflammation.* 2007;30(6): 189-197.
42. Power CP, Wang JH, Manning B, et al. Bacterial lipoprotein delays apoptosis in human neutrophils through inhibition of caspase-3 activity: regulatory roles for CD14 and TLR-2. *J Immunol.* 2004;173(8): 5229-5237.
43. Tsutsumi-Ishii Y, Nagaoka I. Modulation of human beta-defensin-2 transcription in pulmonary epithelial cells by lipopolysaccharide-stimulated mononuclear phagocytes via proinflammatory cytokine production. *J Immunol.* 2003;170(8):4226-4236.
44. Craig FE, Foon KA. Flow cytometric immunophenotyping for hematologic neoplasms. *Blood.* 2008; 111(8):3941-3967.
45. Gorczyca W. Flow cytometry immunophenotypic characteristics of monocytic population in acute monocytic leukemia (AML-M5), acute myelomonocytic leukemia (AML-M4), and chronic myelomonocytic leukemia (CMML). *Methods Cell Biol.* 2004;75:665-677.
46. Maynadie M, Picard F, Husson B, et al. Immunophenotypic clustering of myelodysplastic syndromes. *Blood.* 2002;100(7):2349-2356.
47. Lacronique-Gazaille C, Chaury MP, Le GA, et al. A simple method for detection of major phenotypic abnormalities in myelodysplastic syndromes: expression of CD56 in CMML. *Haematologica.* 2007;92(6): 859-860.
48. Xu Y, McKenna RW, Karandikar NJ, Pildain AJ, Kroft SH. Flow cytometric analysis of monocytes as a tool for distinguishing chronic myelomonocytic leukemia from reactive monocytosis. *Am J Clin Pathol.* 2005;124(5):799-806.
49. Lin Y, Gustafson MP, Bulur PA, et al. Immunosuppressive CD14+HLA-DR(low)/- monocytes in B-cell nonHodgkin lymphoma. *Blood.* 2011;117(3): 872-881.
50. Ellery PJ, Tippett E, Chiu YL, et al. The CD16+ monocyte subset is more permissive to infection and preferentially harbors HIV-1 in vivo. *J Immunol.* 2007;178(10):6581-6589.